Article

Effects of climatic parameters on *Tetranychus urticae* (Acari: Tetranychidae) populations based on remote sensing in the southeastern Caspian Sea

Mahmoud Jokar🔟

Cotton Research Institute of Iran, Agriculture Research, Education and Extension Organization (AREEO), Gorgan, Iran;
E-mail: m.jokar@areeo.ac.ir

ABSTRACT

Tetranychus urticae Koch (Acari: Tetranychidae) is known to be a serious pest in cotton fields worldwide. In this research, monitoring of *T. urticae* was done based on satellite data by using the time series of vegetation index and climatic factors through near real-time assessment. The current study aimed to determine correlations between the population dynamic of *T. urticae* and the effects of Absorbing Aerosol Index (AAI) depicted by Sentinel-5 Precursor, Sentinal-2 NDVI (10 m), Land Surface Temperature (LST), MODIS-Evapotranspiration (ET), and CHIRPS precipitation. Spider-mite outbreak was found to be coincided with wheat harvesting where several dusty days were experienced with a high aerosol index of 0.167. Rainfall had a significant negative correlation with *T. urticae* populations ($R^2 = 0.378$), while a threshold precipitation level of at least 2 mm was estimated for cleaning up the canopy. No significant pattern could be found between temperature and *T. urticae* populations until August 2020. Yet, significant positive relationships were weekly observed during August 2020 ($R^2 = 0.3519, 0.1283, 0.1675$, and 0.178). Evapotranspiration (ET) displayed a statistically synchronous relationship with *T. urticae* dynamism ($R^2 = 0.637$). Also, there was a positive correlation between increasing NDVI and *T. urticae* population until August 2020 and then, it changed to a negative pattern ($R^2 = 0.273$ and 0.139). Based on these findings, AAIs of Sentinel-5 and MODIS-evapotranspiration had the potential to forecast spider-mite population with high temporal resolution.

KEY WORDS: Absorbing Aerosol Index; Evapotranspiration; NDVI; remote sensing; Sentinel-2 and 5; two-spotted spider mite.

INTRODUCTION

Tetranychus urticae Koch (Acari: Tetranychidae), is a serious economic pest in cotton fields worldwide because of its polyphagous behavior accompanied by a wide range of plant hosts (about 900 plant species) (Brown *et al.* 2017). The main spider mite species, including *Tetranychus turkestani* Ugarov & Nikolski and *T. urticae*, are known as a common pest for cotton fields (Forghani and Honarparvar 2012). *Tetranychus urticae* populations have extended in cotton fields in all the territories of Iran, including Golestan, Tehran, Azerbaijan, Khorasan, Ardebil, and Fars provinces (Honarparvar *et al.* 2012). Yield loss caused by two spotted spider mite (*T. urticae*) infestation on cotton, *Gossypium hirsutum* L. (Malvaceae), has been measured in various studies, some of which have tried to determine the two-spotted spider mite populations and the injury levels during 2010 and 2011 (Scott *et al.* 2013).

Among abiotic parameters, climatic parameters such as temperature, relative humidity, rainfall, daytime duration, etc., play a key role in pest population dynamics. Climate factors have been found to affect acarid biology not only mite species such as *Oligonychus coffeae* Nietner (Acari: Tetranychidae) and *Varroa destructor* Anderson & Trueman (Acari: Varroidae) (Ahmed *et al.* 2012; Giliba *et al.* 2020), but also tick species (Gray *et al.* 2009; Liu *et al.* 2016). A 14-year-long population study on Scabies in Taiwan can be mentioned as a typical example which indicted negatively and positively correlated realtionships between scabies population with temperature and humidity, respectively (Liu *et al.* 2016). Also, a 5-year systematic sampling program in Bangladesh aimed at studying the effects of climatic parameters on the Red Spider Mite, *O. coffeae* (Acari: Tetranychidae), which showed its positive responses to temperature, relative humidity, and daytime duration and negative responses to rainfall and cloud coverage (Ahmed *et al.* 2012). The demographic parameters of spider mite pests, e.g. the intrinsic rates of increase (r_m) in *T. pacificus* and *Eotetranychus willamettei* (McGregor) (Acari: Tetranychidae) (Stavrinides and Mills 2011), as well as the parameters of developmental time, sex ratio, and fecundity of *T. urticae* (Margolies and Wrensch 1996), were observed to be temperature-dependent. *Tetranychus urticae* population was found to positively and negatively correspond with mean temperature and mean humidity, respectively (Kumral and Kovanci 2005). According to the targets of the Paris Agreement (1.6 °C warming by 2050) and the suitability modeler of Areas Equipped with Irrigation (AEI) facilities based on climate change, unsuitable conditions for tomato production and a globally increasing risk of two-spotted spider mite outbreak was predicted because of failure in biological control until 2050 (Litskas *et al.* 2019).

Therefore, climatic conditions can affect pest population dynamics, especially in large-scale climate change projections. This can be evidenced through reflectance spectroscopy in the two common ways of using satellite data and an Unmanned Aerial Vehicle (UAV) system equipped with multispectral imagery. The regions infested by *T. urticae* were identified via diffuse reflectance spectroscopy (Visible/Near Infrared Reflectance Spectroscopy) and its damages to strawberries were quantitatively assessed using partial least squares (PLS) regression between mite density and Spectral classification (Fraulo *et al.* 2009). Some researches like Reisig and Godfrey (2006), have reported that the cotton infested by aphid (*Aphis gossypii* Glover) and spider mite (*Tetranychus* spp.) could be distinguished from healthy plants through aerial and satellite images. Martin and Latheef (2017) performed an evaluation by using a ground-based multispectral optical sensor for detecting spider mite damage to cotton in greenhouse conditions. Moreover, supervised classification approaches, such as Support Vector Machine (SVM) and transfer Convolutional Neural Network (CNN), were reported by Huang *et al.* (2018) to be useful for detecting mite infestation using UAV-based multispectral imagery. Furthermore, species composition was specified for modeling ecological niche of tetranychoid mites (Acari: Tetranychoidea) by applying GIS and remote sensing approaches in the different climates of Tehran Province, Iran (Ghasemi Moghadam *et al.* 2016). The current study aimed to determine the potential effects of five climate and vegetation characters, including air pollution (dust), Normalized Difference Vegetation Index (NDVI), Land Surface Temperature (LST), Evapotranspiration (ET), and precipitation, on spider mite population.

MATERIALS AND METHODS

To reveal the relationship between spider mite populations and climatic factors, relative mite density was recorded simultaneously on Saturday in all 65 fields (synoptic recorded spider-mite population, all experts simultaneously recorded the mite population on Saturday). Thematic climatic maps inducing precipitation (mm), MODIS Land Surface Temperature (LST) (MOD11A1, 1 km), Evapotranspiration (kg/m2/8day), Vegetation Index (NDVI) and Aerosol Index (AAL) were provided using Google Earth Engine (GEE) platform. Afterwards, the correlations were examined by extracting 200 random points with Google Earth Engine (GEE) (Fig. 1).

Study area

The study area represented the unique climatic conditions of the northeastern Caspian Sea, including those of the Hyrcanian forest (southern area), deserts (northern area), and fertile lands and vast paddy fields (central area), with 14 adjacent districts (Fig. 2) with the latitude of 36° 30' to 38° 10' N and a longitude of 53° 50' to 56° 20' E.
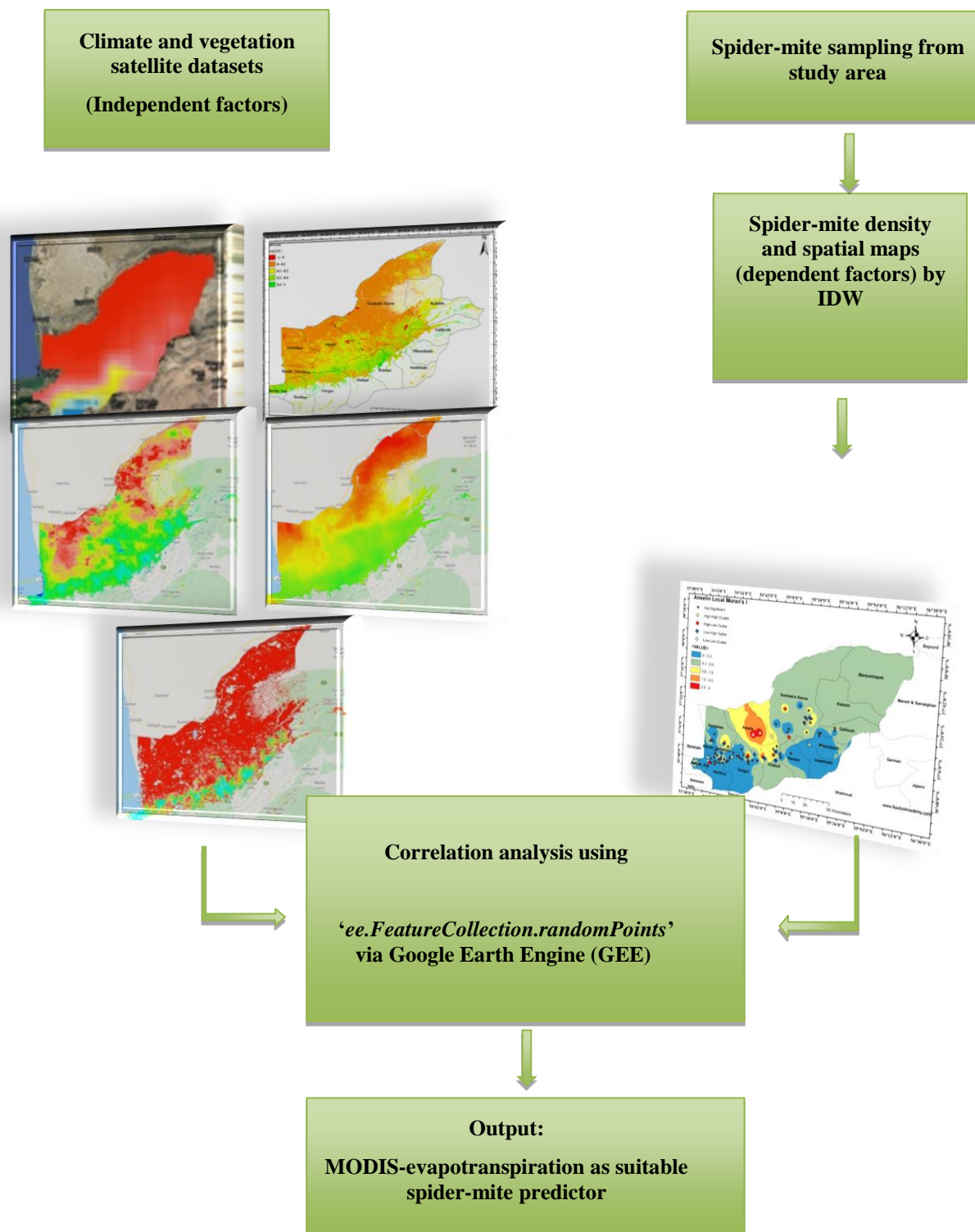

Figure 1. Workflow for examination the relationships between the five parameters and the distribution mite maps.

EFFECTS OF CLIMATIC PARAMETERS ON TSSM POPULATION BASED ON REMOTE SENSING

The climatic effects on the hotspot formation of spider mites could be detected through the climatic diversity of the study area, which covered an area of approximately 21400 km^2 with an altitude ranging from −39 to 3780 m above sea level. Its average annual temperature and precipitation were recorded to be 16.88 °C and 454 mm, respectively. Wheat, barley, canola, and broad bean are their most important autumn crops and soybean, cotton, rice, and sorghum are the major summer crops in this province (Kamkar *et al.* 2014, 2019). Golestan province is one of the top three cotton-producing provinces in Iran (Kamkar *et al.* 2014). Our research covered all the agricultural areas cultivating cotton within this province. The highest areas under cotton cultivation belonged to Aqqala (33%), western part of Gonbad-e-Qabous (31%), and Gorgan (10%), while this crop was barely seen in Minoodasht and Maravehtappeh. To achieve more accurate data, all the satellite images were masked by slope ≥ 3° of the Shuttle Radar Topography Mission (SRTM, 30 m) (Farr *et al.* 2007). The mask areas included highly dense forests (Hyrcanian forests), which are not the ecological niche of *T. urticae*.
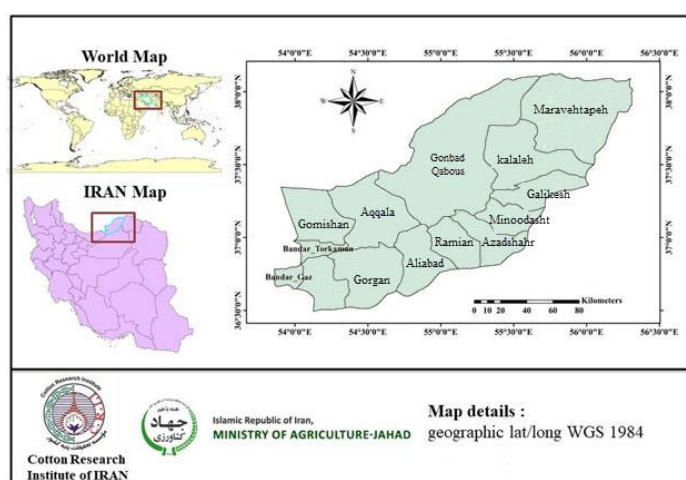

Figure 2. Location of the study area on the world (Golestan province, Iran).

Climate and vegetation datasets as independent factors
Precipitation
As one of the reliable precipitation datasets, the Climate Hazards Group Infrared Precipitation with Stations (CHIRPS) globally provided us with a high resolution of precipitation through interpolation approaches (around 0.05°) for a long period (daily from 1981 to the present time) based on infrared Cold Cloud Duration (CCD), Image Collection ID on Google Earth Engine (GEE), cloud-based image processing platform, and "UCSB-CHG/CHIRPS/DAILY" (Funk *et al.* 2015).

Land Surface Temperature (LST)
The Terra-MODIS Land Surface Temperature (LST) (MOD11A1, 1 km) manipulated by Google Earth Engine (GEE) provided daily information from 09/06/2020 to 17/09/2020. For all the 15 monitoring windows (Table 1), LST time series presented the mean temperatures (day/night) of LST for every window.

Evapotranspiration (ET)
Net Evapotranspiration (ET) was provided by the Evapotranspiration/Latent Heat Flux (MOD16A2/V6) with the productivity of an 8-Day Global 500 m. The algorithm embedding the MOD16 data collection was based on the Penman-Monteith equation (Allen 1996), which was a combination of different input sources, including daily meteorological reanalysis data, vegetation

property, albedo (light surfaces reflect more heat than dark surfaces), and MODIS-land cover (global supervised classification map which highlight different type of vegetation).

Table 1. Monitoring windows for synoptic recorded spider-mite population

Monitoring windows	Date range
W1	May 30, 2020–June 9, 2020
W2	June 9, 2020–June 17, 2020
W3	June 17, 2020–June 24, 2020
W4	June 24, 2020–June 30, 2020
W5	June 30, 2020–July 8, 2020
W6	July 8, 2020–July 15, 2020
W7	July 15, 2020–July 21, 2020
W8	July 21, 2020–July 29, 2020
W9	July 29, 2020–August 3, 2020
W10	August 3, 2020–August 11, 2020
W11	August 11, 2020–August 18, 2020
W12	August 18, 2020–August 29, 2020
W13	August 29, 2020–September 5, 2020
W14	September 5, 2020–September 10, 2020
W15	September 10, 2020–September 17, 2020

The Normalized Difference Vegetation Index (NDVI)

The Normalized Difference Vegetation Index (NDVI) is one of the most applicable vegetation indices in remote sensing projections (Lamqadem *et al.* 2018). NDVI is worked on the red and NIR reflectance of an object. Its values are within the range of −1 (water resources and snow body) and +1 (full vegetation coverage). In the current research, the 7–10-day multi-temporal Sentinal-2 data were provided by NDVI index during monitoring the windows.

Air pollution (aerosol index)

The "NRTI/L3_AER_AI" dataset from Sentinel-5 provides near real-time high-resolution imagery of the UV Aerosol Index (UVAI) or Absorbing Aerosol Index (AAL). This index works according to the wavelength-dependent changes in Rayleigh scattering in the UV spectral range for a pair of wavelengths, i.e., 354 and 388 nm. A positive AAI indicates the presence of those phenomena that can absorb UV, like dust and smoke. The pair of selected wavelengths are very lowly absorbed by ozone (Soleimany *et al.* 2021).

Spider mite sampling and spatial analysis as dependent factors for drawing the distribution map of T. urticae

Spider mite sampling as the ground-truth data

The ground-truth data of spider-mite population were reported via mean percentage of the leaf area infected with various symptoms of spider mite (dust-silk webbing, yellow spots, etc.). One hundred cotton leaves were randomly observed by our experienced experts, who estimated the infestation scores of spider mite in each field according to the following formula.

$$(1) \textbf{\textit{Infestation rate}} = \frac{(n_i \times p_i) + (n_j \times p_j) + (n_l \times p_l) + \cdots}{100}$$

Where *n* and *p* are the number of leaves and their infestation percentage, respectively, and *i*, *j*, *l* etc. indicate the same infestation percentages. For the unity of procedure, the estimated percentages of infestation were reported based on specific intervals, including 0 for no evidence of spider mite,

and 1–10 %, 11–20 %, 21–30 %, 31–50 %, and $\geq$ 50 % of infested leaf area, respectively. In this research, the data collected from 65 cotton fields throughout Golestan province were utilized based on the grid cells of 6 (min.) $\times$ 6 (min.) in the Degree/Minute/Second (DMS) coordinate system (Fig. 3). Measurements in these fields were based on the percentages of spider mite involvement during a fixed time. Afterwards, the distribution maps of spider mite were spatially analyzed for 15 monitoring windows via Inverse Distance Weighted (IDW) interpolation by using ArcMap/GIS 10.6 software. The deterministic interpolation method was applied to 'Spatial Analyst Tools' in ArcMap software package (version 10.6, ESRI, Redlands, CA) to draw the spider mite distribution maps using the collected data. This process was performed in every monitoring field located inside a grid cell.
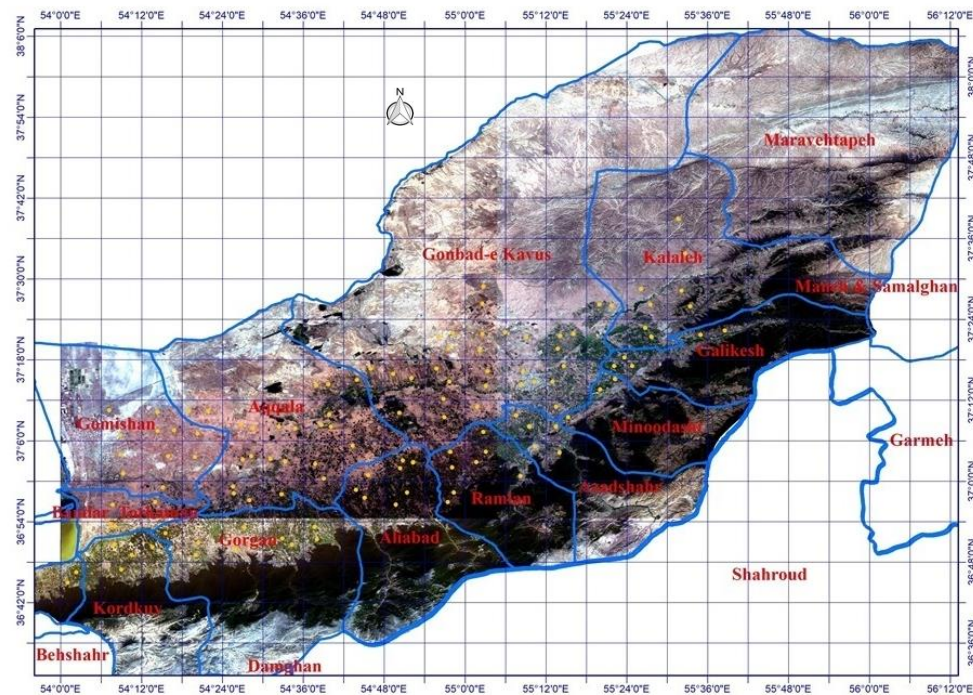

Figure 3. Spider mite distribution throughout Golestan province; 6 (min.) $\times$ 6 (min.) grid cells in the DMS coordinate system (yellow points indicate the monitoring fields).

Regression analysis

Various satellite data, such as AAL index of Sentinel-5P, LST-MODIS (Terra), NDVI-Sentinel–2, CHIRPS, and ET-MODIS, were assessed as the main independent factors for spider mite outbreak. For each window, 200 random points were extracted to assess the correlation between an interpolation map of spider mite (dependent factor) and 5 satellite-based parameters (independent factors) by using '*ee.FeatureCollection.randomPoints*' via Google Earth Engine (GEE) platform. The relationships between the 5 parameters and the distribution windows maps were statistically examined using ANOVA regression analysis in SPSS software (version 23).

Spatial autocorrelation

Moran's Index has been known as a more applicable statistic for spatial autocorrelation. Global Moran's I can estimate the possibility of spatial correlation at the study region. The amplitude of fluctuations in the Moran's I values is between 1 and −1. Positive autocorrelation (clustered) and negative autocorrelation (dispersed) in the data are translated into the positive and negative values of Moran's I, respectively. The random distribution of a variable (no autocorrelation) results in a value close to 0 (Overmars *et al.* 2003). The relationship between a pixel and its surrounding pixels is

estimated by weight matrix. Therefore, a distance-based weight matrix (a threshold distance of 5000 m) was applied to consider the "neighbors" (just non-zero values) for all the pixels located at a certain distance. The normal approximation for global Moran's I could be standardized to $Z(I)$ and $Z(I)$ (Legendre and Fortin 1989). The significance level of $Z(I)$ was a threshold (1.96) so that the spatial autocorrelation could be regarded significant if $Z(I)$ fluctuated between 1.96 and −1.96 (Zhang and McGrath 2004). The spatial correlogram showed patterns of spatial autocorrelation when the distances between the observations increased. The spatial correlogram was drawn in two common forms, including Moran's I or $Z(I)$ (standardized Moran's I) (Legendre and Fortin 1989), which were plotted as ordinate against distance as abscissa although the standardized correlogram represented the spatial distance correlation that was the first positive peak (Zhang *et al.* 1998). Local Moran's I is computed to identify locations of spatial clusters and outliers (Anselin 2010). In the analysis of local Moran's I, there are 5 possibilities for local spatial autocorrelations. Two types of them distinguish spatial clusters, including high values surrounded by high values (high-high) and low values surrounded by low values (low-low). Two other types are known as outliers, including high values surrounded by low values (high-low) and low values surrounded by high values (low-high). Finally, the last value is plotted as a non-significant spatial pattern (spatial randomness).

Geostatistical method

In the grid system, the classical IDW interpolation method had the lowest Root Mean Square Error (RMSE) in pre-evolution (Gorgan data) compared to those of the other methods. It was used to build the abundance maps, which were consistent with the results obtained by Al-Kindi *et al.* (2017). Through IDW method, the values of an unknown pixel are estimated by the predicted nearby pixels though restricted in the range of maximum and minimum values of the true pixels. The Nearest Neighbor Statistical (NNS) analysis spatially detected statistical moth distribution, including absence, random, regular, or aggregation possibilities in each area (Vinatier *et al.* 2011).

RESULTS AND DISCUSSION

Spatial pattern analysis of spider mite using the spatial autocorrelation analysis

Generally, a higher Moran's I in the absolute value represents a greater spatial correlation and a more significant spatial autocorrelation is shown by a higher standardized form of Moran's I, Z(I), which is able to compare the statically spatial patterns of different phenomena or different calculating parameters of the same phenomenon. At the global autocorrelation, Table 2 depicts the first three windows (there were no data for spider-mite population in the first window), which do not show a significant correlation (random distribution) for the standardized form of global Moran's I (≥ 1.96). The 4th window was at a significant level during June of 2020. During the studied periods, the cotton plants did not complete the canopy, but they were symmetrical with the wheat harvesting calendar at the 4th window in Golestan province. Wheat harvesting causes huge local dust. After that, a sinusoidal pattern was seen in the global autocorrelation (randomness to aggression, vice versa) (Table 2). By beginning of August 2020 (the 9th and 11th windows), the study areas faced a spider mite outbreak and the strongest spatial structure was evidenced (Fig. 4h, i). The descending spatial structures at the 10th, 13th, and 14th windows could be related to pesticide application at the cotton fields.

Figure S1 represents the standardized spatial correlograms of spider mite distribution at all the monitoring windows (15 windows). The Moran's I and standardized Moran's I, Z(I), reached their maximum values at the threshold distance of the weight matrix. At the 1st window (May 30, 2020– June 9, 2020), no spider mites were observed in the pilot farms and thus, no data were reported by the local experts. The positive standardized Moran's I values at the distance of 5–15 km indicated the spatial clusters of similar spider mite populations. Generally, the optimal distance was 10 km to reach the maximum value of Moran's I for detecting a local spatial pattern. The interpolation maps of spider

mite population were drawn using the IDW method through cross-validation of the parameters. The evaluation indices obtained from cross-validation of the IDW maps for all the monitoring windows are given in Table 3 and Figure S2.

Table 2. Spatial global autocorrelation of spider mite population at monitoring programs, Dispersed [$Z(I)^{**} < -2.58$; $-2.58 \leq Z(I)^* \geq -1.96$; p-value = 0.1, $-1.96 \leq Z(I) \geq -1.65$], Random [$-1.96 \leq Z(I)^{ns} \geq -1.65$], Clustered [$Z(I)^{**} > -2.58$, $1.96 \leq Z(I)^* \geq 2.58$; p-value = 0.1, $1.65 \leq Z(I) \geq -1.96$].

period	Global Moran's Index	Z-score	p-value	pattern
Window_1	No Data	No Data	No Data	No Data
Window_2	0.029207	0.731330	0.464578	Random
Window_3	−0.003930	0.107097	0.914712	Random
Window_4	0.247838	3.871930	0.000108	Clustered
Window_5	0.053822	1.018388	0.308494	Random
Window_6	0.043046	0.961567	0.336267	Random
Window_7	0.096227	1.789161	0.073589	Clustered
Window_8	0.076148	1.641488	0.100696	Random
Window_9	0.337405	6.283151	0.000000	Clustered
Window_10	−0.009247	−0.016164	0.987104	Random
Window_11	0.262986	6.777026	0.000000	Clustered
Window_12	0.217330	4.373817	0.000012	Clustered
Window_13	0.039474	0.991156	0.321610	Random
Window_14	0.042141	1.339547	0.180393	Random
Window_15	0.264988	5.138441	0.000000	Clustered

Table 3. Evaluation indices of the interpolation maps (IDW) of spider mite distribution during monitoring program.

period	equations	RMSE
Window_1	No data	No data
Window_2	$0.029 \times x + 0.023$	0.3556
Window_3	$0.018 \times x + 0.1086$	0.5555
Window_4	$0.035 \times x + 0.116$	0.4650
Window_5	$0.063 \times x + 0.284$	0.62478
Window_6	$0.035 \times x + 0.201$	0.7948
Window_7	$0.0557 \times x + 0.209$	0.6404
Window_8	$0.091 \times x + 0.161$	0.6792
Window_9	$0.255 \times x + 0.102$	0.534
Window_10	$0.0279 \times x + 0.239$	1.009
Window_11	$0.066 \times x + 0.257$	0.891
Window_12	$0.137 \times x + 0.259$	0.893
Window_13	$0.032 \times x + 0.239$	1.054
Window_14	$0.012 \times x + 0.25$	0.919
Window_15	$–0.008 \times x + 0.071$	0.6030

Cross-validation of the spatial interpolation confirmed the accuracy of the estimated model. The common parameters, which could measure errors, included Mean Error (ME), Mean Absolute Error (MAE), Mean Squared Error (MSE), and Root Mean Squared Error (RMSE). RMSE, which is sensitive to outliers, is known as an optimal model evaluator capable of measuring error size (Willmott 1982; Hernandez-Stefanoni and Ponce-Hernandez 2006). The smaller RMSE indicated that the semivariogram parameters calculated by fitting the experimental values were suitable and the geostatistical prediction had worked more accurately. According to the interpolation maps of spider

mite distribution, some regions struggled with high population densities of *T. urticae* (Fig. 4). The infestation patterns of *T. urticae* revealed the temporal hot spots in the central and eastern areas of Golestan province where the mechanized harvesting of grains was associated with dust pollution (Fig. 4 b–f). Upon establishing spring and summer crops like cotton in late July, the patterns of *T. urticae* changed towards other regions of the study areas. In the 8th window (July 21, 2020–July 29, 2020), Aqqala city was the main area of *T. urticae* (Fig. 4g). This finding was confirmed by the Agriculture Administration, which named Aqqala as the niche of *T. urticae* at Golestan Province. At the 15th window, *T. urticae* population declined sharply because of completion of the growing season of cotton and arrival of the harvest dates (Fig. 4n). The spatial analysis of *T. urticae* during the growing season of cotton revealed several ups and downs in *T. urticae* populations, but the climatic aspects influencing this pattern still remained hidden. Based on the empirical observations, climatic variables, especially aerosol and dust in the air, had significant impacts on *T. urticae* population.
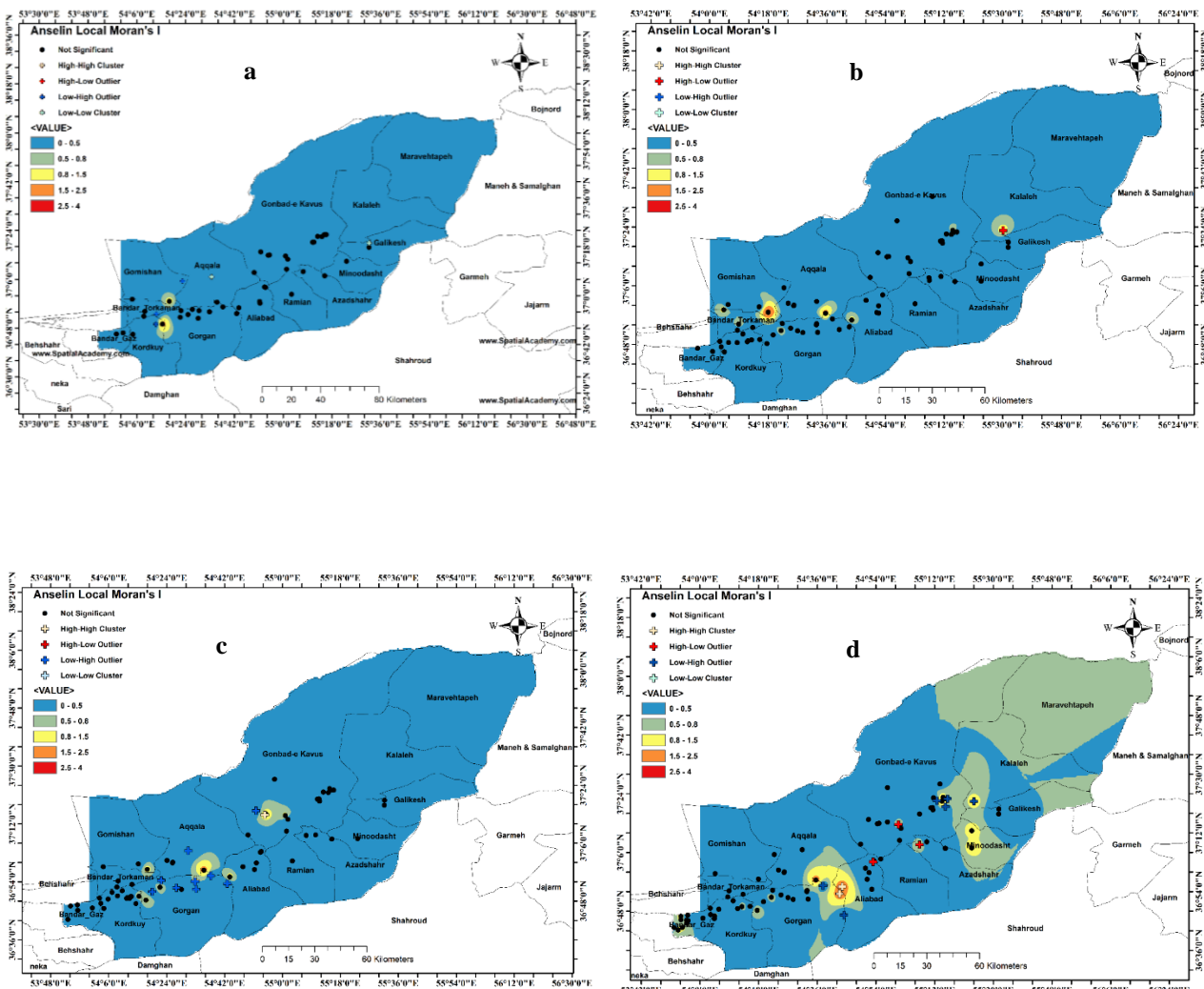
Figure 4. Distribution maps of spider mite based on IDW model during monitoring windows, a–n are the sequence windows form June 9, 2020 to September 17, 2020 (First window, May 30 to June 9 was not spider mite population data).
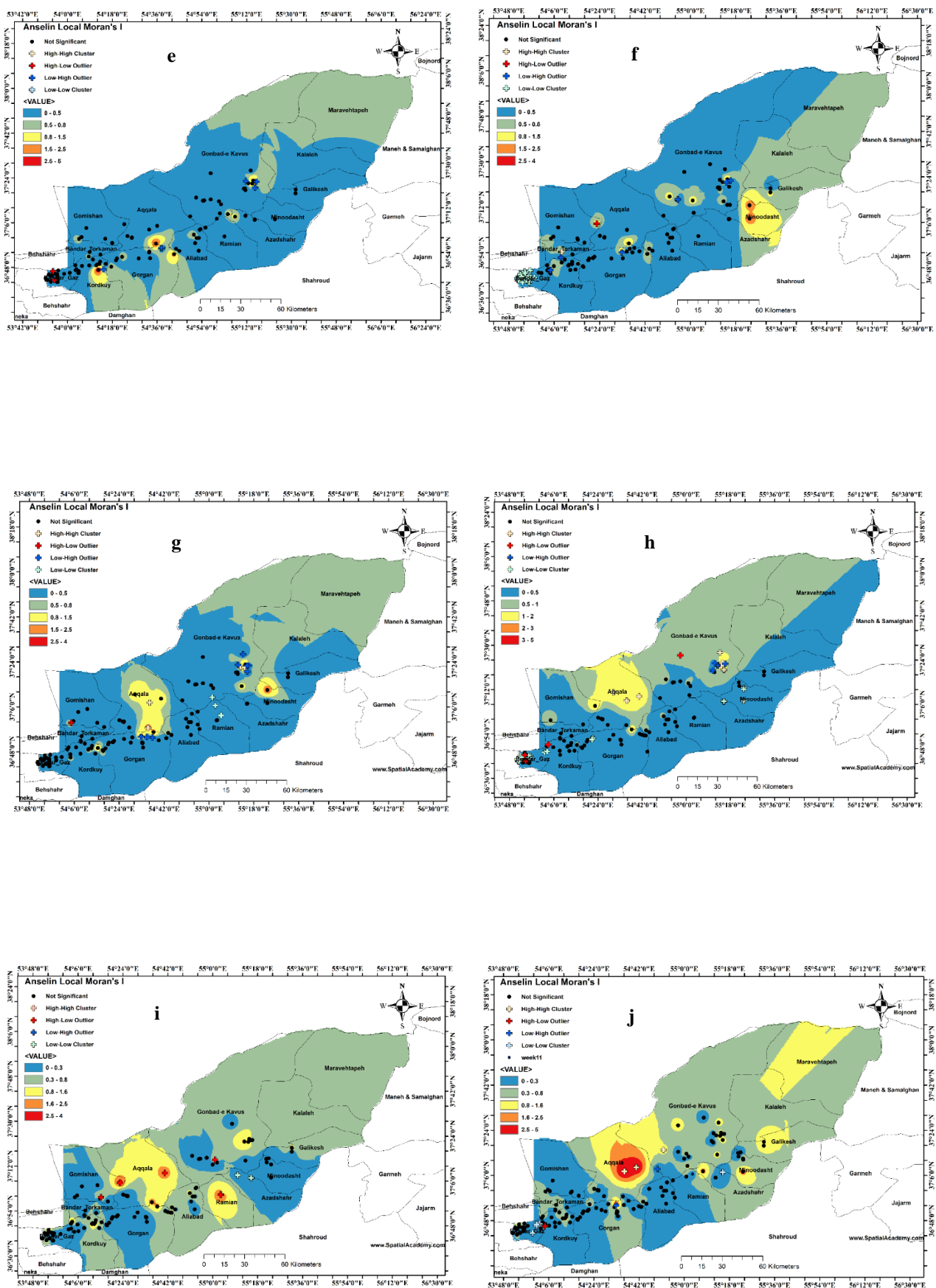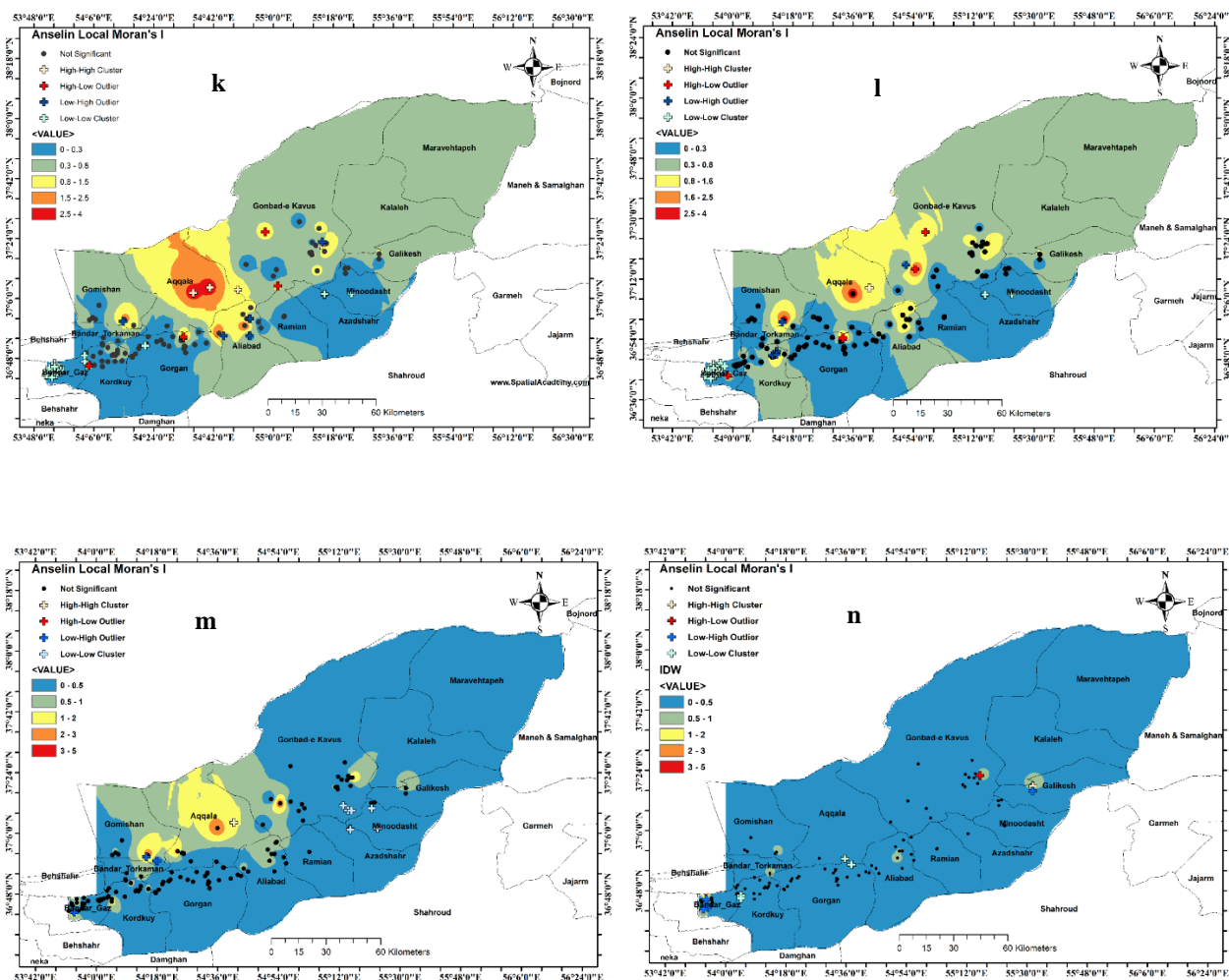
Figure 4. Continued.

Figure 4. Continued.

Effects of climatic factors on spider mite population

　　As mentioned before, there were not enough canopies to establish *T. urticae* on the cotton fields up to the 5th window (Fig. 4d), after which the spider mite outbreak coincided with the wheat harvest and a high aerosol index of 0.167 on the 21st of June, 2020. In the first three windows, the study area experienced several dusty days and faced the 1st peak of *T. urticae* population (Figs. 4d, 5). The statistically tight relationship between dusty days and spider mite was repeated in the transition mode from the 9th and 13th windows to their next windows (from w9 to w10 and w13 to w14) (Fig. 5). The effects of dust and different environmental conditions on spider mites were reported in several studies (Hodek 1987; Thomas 2001; Guerena and Sullivan 2003). The results of the previous studies conducted by Flint (1998) and Guerena and Sullivan (2003) supported those of the present research. The mentioned studies also represented that the dusty conditions almost caused an increase in *T. urticae* populations on farms. According to the findings obtained by Demirel and Cabuk (2008), spider mite densities were 1.72, 1.75, 4.39, and 2.65 times higher on cotton farms in the vicinity of dirt roads compared to asphalt roads. Therefore, dust removal could be considered as an applicable approach to the proper production of organic cotton (Guerena and Sullivan 2003) by controlling *T. urticae* population using insecticidal soaps and through water washing to achieve complete coverage. The effects of precipitation that has the ability to remove dust on cotton canopies and control *T.*

urticae populations are presented in Figure 6. In the 1st window, the hidden impact of rainfall on lowering *T. urticae* population could be observed along with about 2.5 mm/day precipitation resulting in a low density canopy in this period. This negative relationship was repeated in the 9th and 12th windows (approximately ≥ 2 mm). Based on current results, the study area would experience a severe outbreak of *T. urticae* during July 2020 even if rain did not fall about 2 mm on July 6 and 16, 2020. The threshold precipitation level was estimated to be at least 2 mm to clean up the canopy. Rao *et al.* (2018) evaluated the impacts of environmental factors on the population dynamics of *T. urticae* in the ecosystem of Brinjal, India, and reported a gradual increase in *T. urticae* population from 4.34 to 32.64 (number of mites present in 2 cm^2 of leaf area), the result of which is in agreement with that of the current study showing an increase from 0.05 to 0.45 scores of spider mite populations. The findings of Rao *et al.* (2018) demonstrated that rainfall (Y = 19.358–1.055X; $R^2 = 0.378$) had a significant negative relationship with *T. urticae* population, which corroborates the negative relationship achieved in the 2nd (y = −1.494 x + 0.3184; $R^2 = 0.2201$), 9th (y = −0.4616 x + 0.6478; $R^2 = 0.1329$), and 12th (y = −0.1428 x + 0.1103; $R^2 = 0.1213$) windows of the current research. The absence of precipitation coupled with a suitable temperature was introduced by Rao *et al.* (2018) as the main environmental factor contributing to the rise in *T. urticae* population. Evaluation of the relationship between spider mite population and temperature averages was another part of our climate studies. The main source of temperature measurement was MODIS-LST imagery twice a day (Fig. 7). We could not find a significant relationship between temperature and *T. urticae* population until August, 2020. Nevertheless, significantly tight relationships were observed in the 9th (y = 8.4748 x + 38.298; $R^2 = 0.3519$; P-value = 0.000), 10th (y = 7.5261 x + 38.43; $R^2 = 0.1283$; P-value = 0.008), 11th (y = 3.7942 x + 33.272; $R^2 = 0.0859$; P-value = 0.041), 12th (y = 6.6459 x + 35.306; $R^2 = 0.1675$; P-value = 0.004), and 13th (y = 6.322 x + 36.522; $R^2 = 0.178$, P-value = 0.002) windows. In many studies, a negative relationship between temperature and spider mite populations has been reported (Majeed *et al.* 2016; Fahim and El-Saiedy 2021). This result is congruent with those obtained by Fahim and El-Saiedy (2021), who reported an insignificant relationship between mean temperature and *T. urticae* populations at the beginning of the growing season. However, there are many findings from the previous literature supporting the positive relationship between *T. urticae* populations and temperature (Meena *et al.* 2013; Chauhan and Shukla 2016). The seasonal abundance of *T. urticae* is influenced by biotic and abiotic factors. Parasitoid and predators are known as the biological factors suppressed by temperature and drought (Romo and Tylianakis 2013). Evapotranspiration (ET) as another parameter of climate was predicted to affect the abundance, distributions, and activities of pests. Increasing ET shows the potential to simulate drought conditions (Mullan *et al.* 2005). The relationship between spider mite populations and ET depicted a statistically strong relationship (mean square = 0.349; F = 21.038, $R^2 = 0.637$; p-value = 0.001) as displayed in Figure 8. This result was similar to the findings of Litskas *et al.* (2019), who reported the relationships of ET with *T. urticae* ($R^2 = 0.46$) and its natural enemy, *P. persimilis* ($R^2 = 0.60$), respectively. Since all the climate factors had their effects on this plant, NDVI could support its correlation with spider mite populations as well. During monitoring the windows, negative and positive relationships between NDVI and spider mite scores were observed. Also, there was a positive correlation between increasing NDVI and *T. urticae* population up to the 10th window (August 2020) (Figs. 9a–g). The 5th and 6th windows (middle of July 2020) demonstrated significant relationships ($R^2 = 0.107$, p-value = 0.016) and ($R^2 = 0.110$, p-value = 0.015), respectively. Beginning in August 2020, there was a shift to a negative relationship, especially in the 9th and 13th windows with $R^2 = 0.273$ (p-value = 0.000) and $R^2 = 0.139$ (p-value = 0.006), respectively. This phenomenon was interpreted by the fact that *T. urticae* had an opportunity to establish its communities through cotton canopy enhancement. After that, the negative correlations were due to *T. urticae* population causing a severe decrease in NDVI (Fig. 9). The NDVI decline caused by *T. urticae* was confirmed by numerous studies aimed at assessing *T. urticae* population and its damages (Lan *et al.* 2013; Martin *et al.* 2015; Martin and Latheef 2017). During multi-temporal

NDVI series, severe reduction of the 11th window (3–11 August, 2020) was observed because of high aerosol density and low rainfall (Fig. 9j).
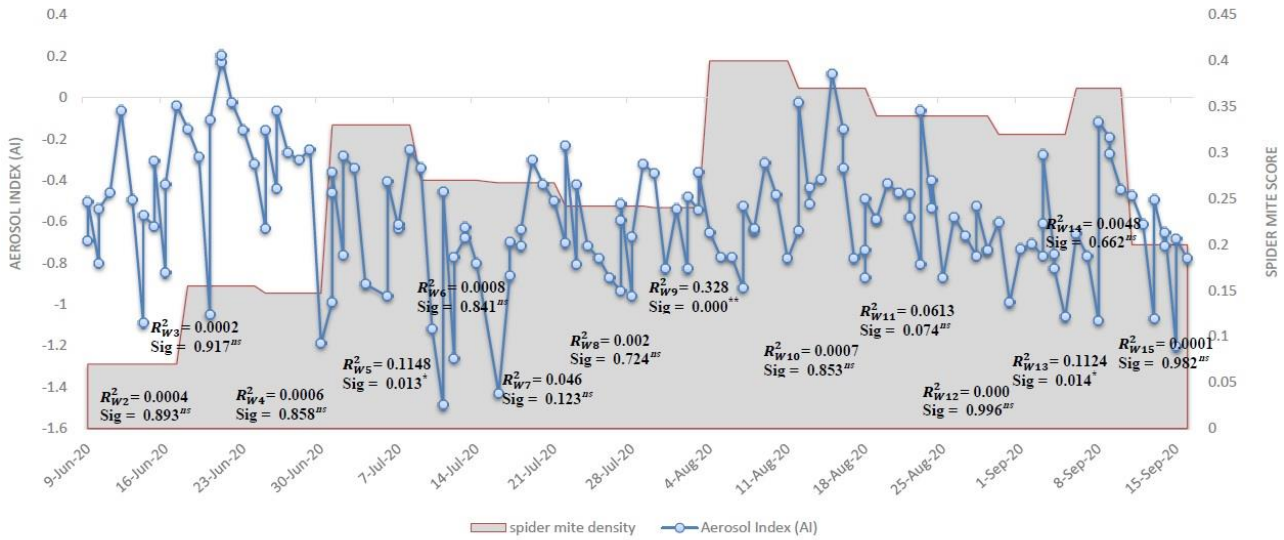

Figure 5. The relationship between UV Aerosol Index extracted from Sentinel-5 imagery and spider mite population (mean score of each window) from June 9, 2020 to September 17, 2020 (First window, May 30 to June 9 was not spider mite distribution data).
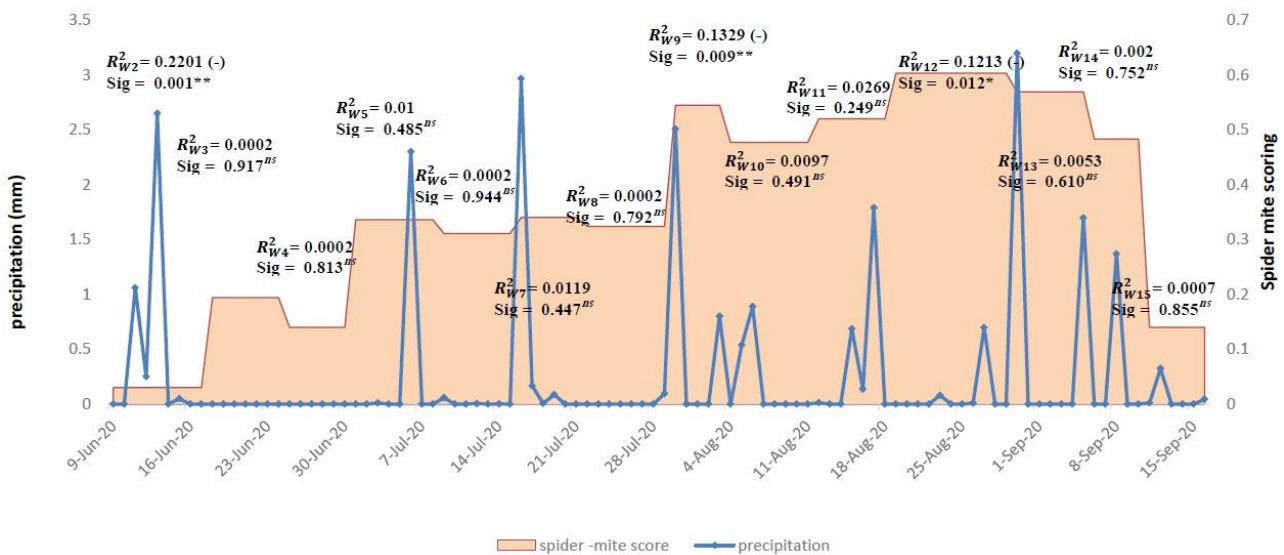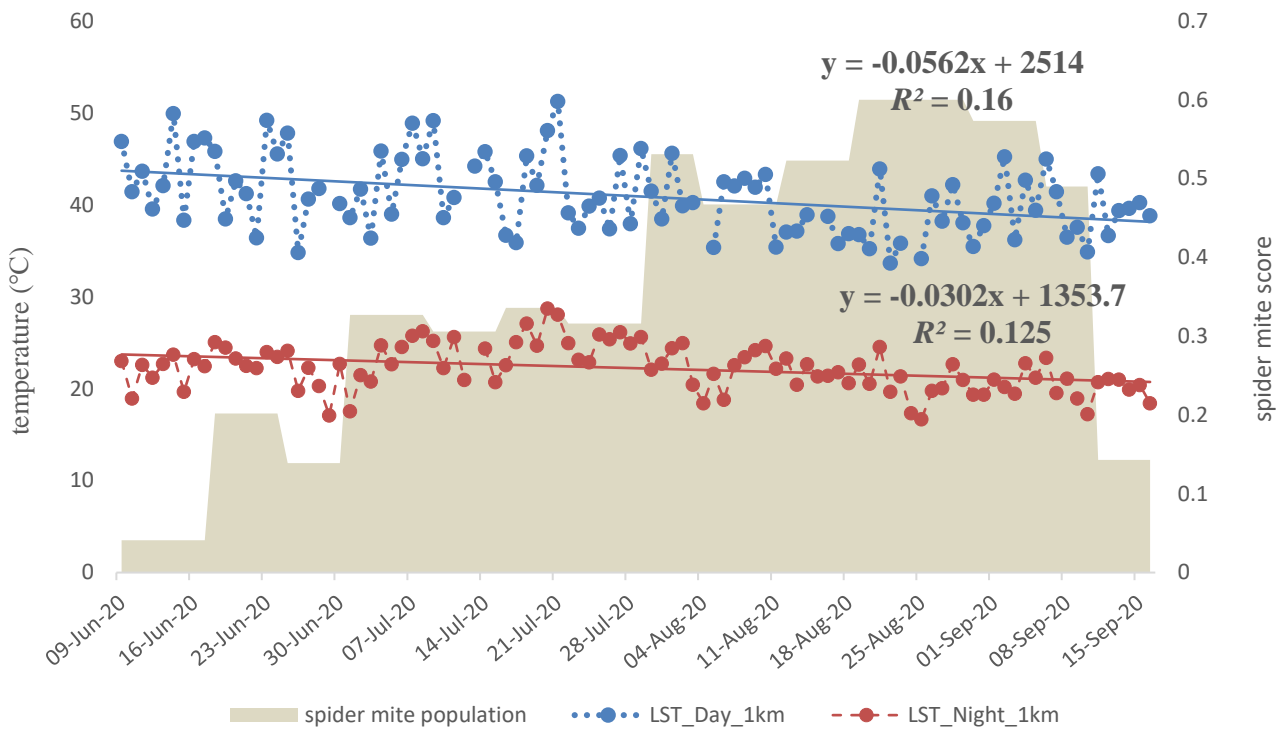

Figure 6. The relationship between daily CHIRPS-precipitation and spider mite population (mean score of each window) from June 9, 2020 to September 17, 2020 (First window, May 30 to June 9 was not spider mite distribution data).

**Figure 7.** The relationship between daily Land Surface Temperature and spider mite population (mean score of each window) from June 9, 2020 to September 17, 2020. (First window, May 30 to June 9 was not spider mite distribution data), … and -- are Day and night LST, respectively.
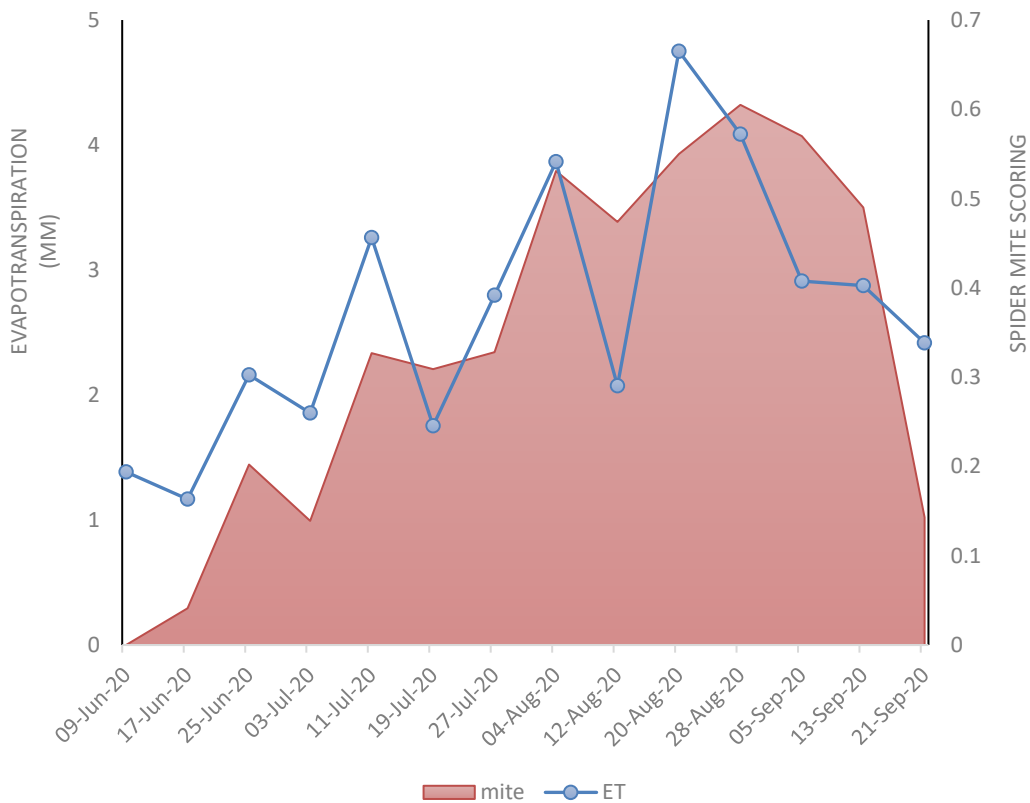
Figure 8. The relationship between MODIS-Evapotranspiration and spider mite population (mean score of each window) from June 9, 2020 to September 17, 2020. (First window, May 30 to June 9 was not spider mite distribution data).

EFFECTS OF CLIMATIC PARAMETERS ON TSSM POPULATION BASED ON REMOTE SENSING
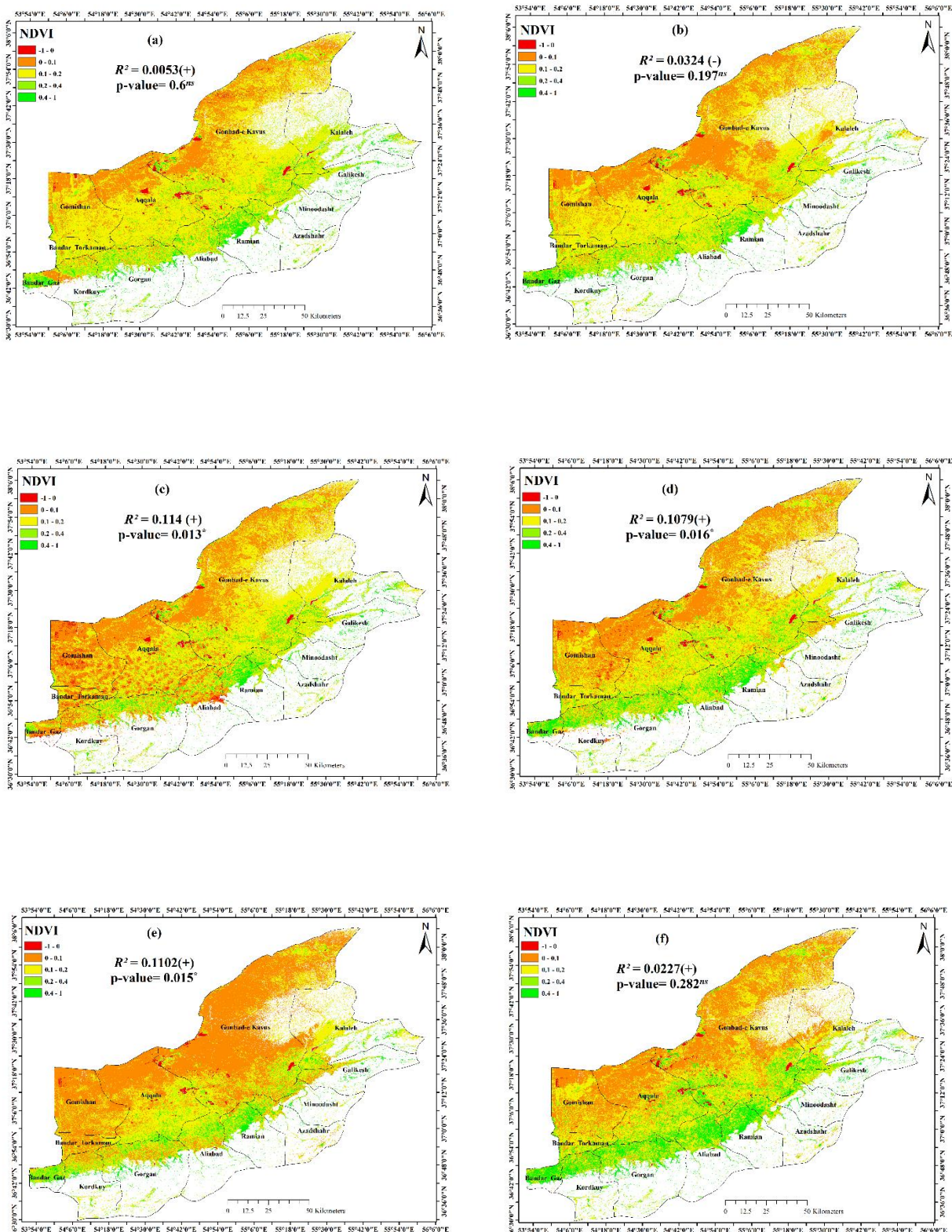
Figure 9. The relationship between NDVI (10 m) provided form Sentinal-2 and density of spider mite during monitoring windows based on ANOVA for linear regression. The alphabetical letters indicate of the sequence windows from June 9, 2020 to September 17, 2020 (First window, May 30 to June 9 was not spider mite distribution data).
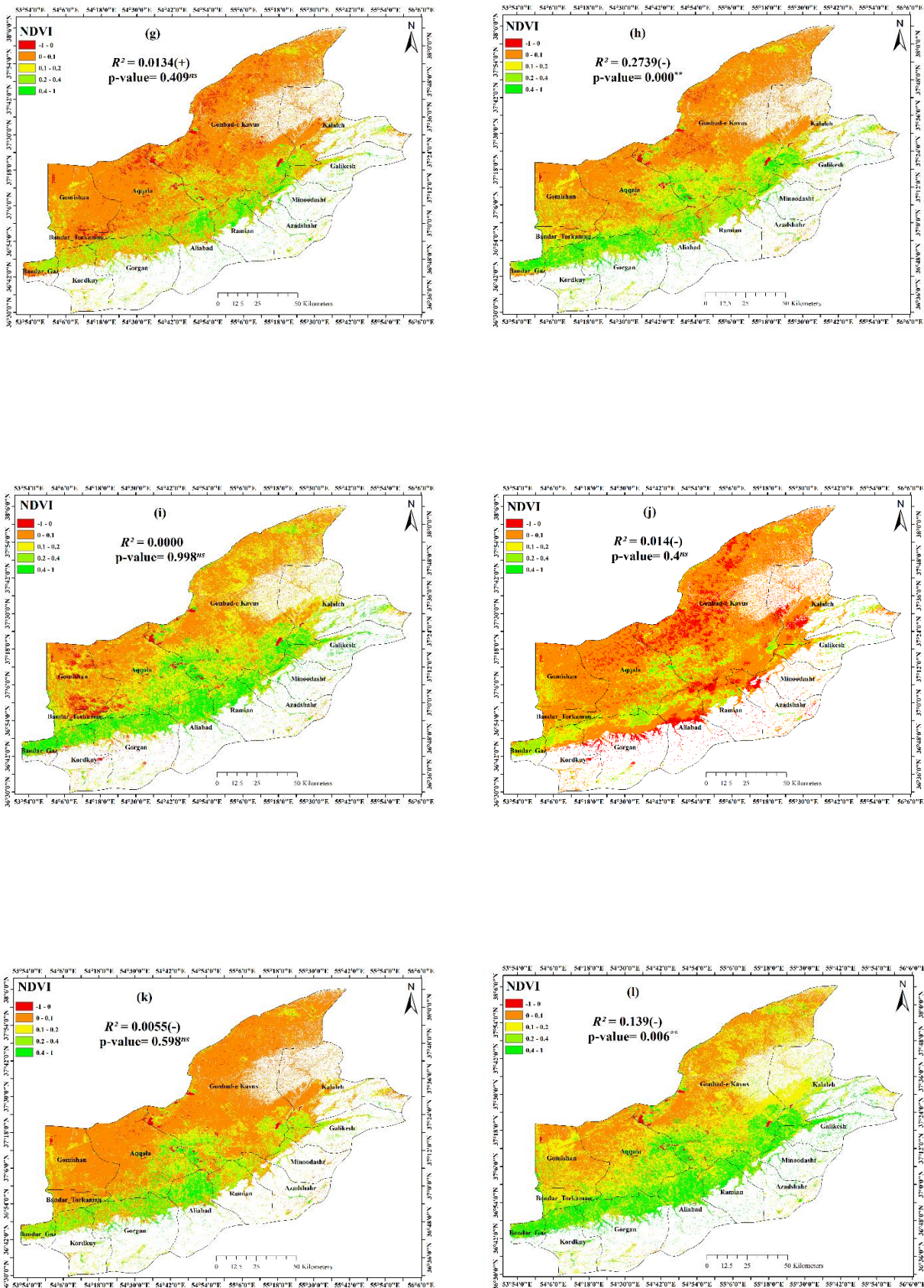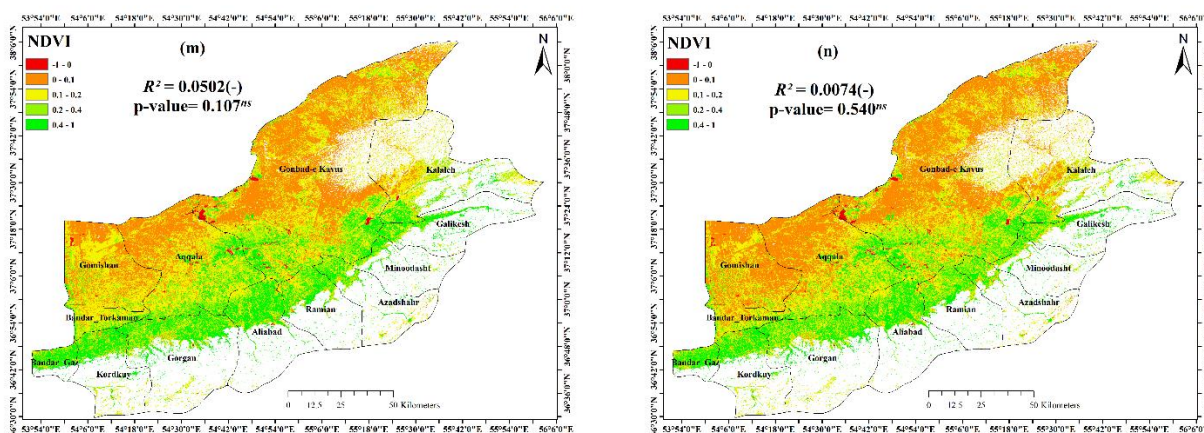
Figure 9. Continued.

Figure 9. Continued.

CONCLUSION

In this investigation, *T. urticae* was found to have diverse responses to climatic factors. Based on a pre-judgment at the beginning of the study, from among the varied climatic factors, aerosol index (dusty days) was predicted to severely influence the spider mite density on the monitoring fields. However, evapotranspiration was seen to be exactly synced to the population dynamic of *T. urticae*. Indeed, sentinel-5 and MODIS-evapotranspiration were evidenced to have a suitable potential to predict spider mite populations with the help of aerosol index with a high temporal resolution. The study of these drivers offers a realistic view of the accurate models experts can design under a regime of climate change.

REFERENCES

Ahmed, M., Mamun, M.S.A., Hoque, M.M. & Chowdhury, R.S. (2012) Influence of weather parameters on Red spider mite- A major pest of tea in Bangladesh. *SUST Journal of Science and Technology*, 19: 47–53.

Al-Kindi, K.M., Kwan, P., Andrew, N. & Welch, M. (2017) Impact of environmental variables on Dubas bug infestation rate: A case study from the Sultanate of Oman. *PLoS ONE* 12: e0178109. DOI: 10.1371/journal.pone.0178109

Allen, R.G. (1996) Assessing integrity of weather data for reference evapotranspiration estimation. *Journal of Irrigation and Drainage Engineering*, 122: 97–106. DOI: 10.1061/(ASCE)0733-9437 (1996)122:2(97)

Anselin, L. (2010) Local Indicators of Spatial Association-LISA. *Geographical Analysis*, 27: 93–115. DOI: 10.1111/j.1538-4632.1995.tb00338.x

Brown, S., Kerns, D.L., Gore, J., Lorenz, G. & Stewart, S. (2017) Susceptibility of twospotted spider mites (T*etranychus urticae*) to abamectin in Midsouth cotton. *Crop Protection*, 98: 179–183. DOI: 10.1016/j.cropro.2017.04.002

Chauhan, R.K. & Shukla, A. (2016) Population dynamics of two spotted spider mite, *Tetranychus urticae* Koch on French bean (*Phaseolus vulgaris* L.). *International Journal of Plant Protection*,

9: 536–539. DOI: 10.15740/HAS/IJPP/9.2/536-539

Demirel, N. & Cabuk, F. (2008) Population trends of two spotted spider mite, *Tetranychus urticae* Koch (Acari: Tetranychidae) on cotton nearby soil and asphalt road. *Journal of Entomology*, 5: 122–127. DOI: 10.3923/je.2008.122.127

Fahim, S.F. & El-Saiedy, E.-S.M. (2021) Seasonal abundance of *Tetranychus urticae* and *Amblyseius swirskii* (Acari: Tetranychidae and Phytoseiidae) on four strawberry cultivars. *Persian Journal of Acarology*, 10: 191–204. DOI: 10.22073/pja.v10i2.63667

Farr, T.G., Rosen, P.A., Caro, E., Crippen, R., Duren, R., Hensley, S., Kobrick, M., Paller, M., Rodriguez, E., Roth, L., Seal, D., Shaffer, S., Shimada, J., Umland, J., Werner, M., Oskin, M., Burbank, D. & Alsdorf, D. (2007) The Shuttle radar topography mission. *Reviews of Geophysics*, 45: RG2004. DOI: 10.1029/2005RG000183

Flint, M.L. (1998) *Pests of the Garden and Small Farm. A Grower's Guide to Using Less Pesticide*. 2nd Edition. UC Division of Agriculture and Natural Resources and University of California, Berkeley, 276 pp.

Forghani, H. & Honarparvar, N. (2012) Determination of the dominant spider mite (Acari: Tetranychidae) species on cotton fields in Golestan province, Iran. *Biharean Biologist*, 6: 116–121.

Fraulo, A.B., Cohen, M. & Liburd, O.E. (2009) Visible/Near Infrared Reflectance (VNIR) spectroscopy for detecting twospotted spider mite (Acari: Tetranychidae) damage in strawberries. *Environmental Entomology*, 38: 137–142. DOI: 10.1603/022.038.0117

Funk, C., Peterson, P., Landsfeld, M., Pedreros, D., Verdin, J., Shukla, S., Husak, G., Rowland, J., Harrison, L., Hoell, A. & Michaelsen, J. (2015) The climate hazards infrared precipitation with stations—a new environmental record for monitoring extremes. *Scientific Data*, 2: 150066. DOI: 10.1038/sdata.2015.66

Ghasemi Moghadam, S., Ahadiyat, A. & Ueckermann, E.A. (2016) Species composition of tetranychoid mites (Acari: Trombidiformes: Prostigmata: Tetranychoidea) in main landscapes of Tehran and modelling ecological niche of Tetranychoidea in main climates of Tehran Province, Iran. *Biologia*, 71: 1151–1166. DOI: 10.1515/biolog-2016-0138

Giliba, R.A., Mpinga, I.H., Ndimuligo, S.A. & Mpanda, M.M. (2020) Changing climate patterns risk the spread of *Varroa destructor* infestation of African honey bees in Tanzania. *Ecological Processes*, 9: 48. DOI: 10.1186/s13717-020-00247-4

Gray, J.S., Dautel, H., Estrada-Peña, A., Kahl, O. & Lindgren, E. (2009) Effects of climate change on ticks and tick-borne diseases in Europe. *Interdisciplinary Perspectives on Infectious Diseases*, 1–12. DOI: 10.1155/2009/593232

Guerena, M. & Sullivan, P. (2003) *Organic cotton production*. NCAT Agriculture Specialists, 24 pp.

Hernandez-Stefanoni, J.L. & Ponce-Hernandez, R. (2006) Mapping the spatial variability of plant diversity in a tropical forest: Comparison of spatial interpolation methods. *Environmental Monitoring and Assessment*, 117: 307–334. DOI: 10.1007/s10661-006-0885-z

Hodek, I. (1987) W. Helle & M.W. Sabelis, Eds (1985). Spider mites. Their Biology, Natural Enemies and Control. *Entomologia Experimentalis et Applicata*, 43: 203–204. DOI: 10.1111/j.1570-7458.1987.tb03606.x

Honarparvar, N., Khanjani, M., Forghani, S.H.R., Ostovan, H. & Talebi, A.A. (2012) Demographic parameters of two spotted spider mite, *Tetranychus urticae* Koch (Acari: Tetranychidae) on cotton. *Archives of Phytopathology and Plant Protection*, 45: 381–390. DOI: 10.1080/03235408.2011.587296

Huang, H., Deng, J., Lan, Y., Yang, A., Deng, X., Zhang, L., Wen, S., Jiang, Y., Suo, G. & Chen, P.

(2018) A two-stage classification approach for the detection of spider mite-infested cotton using UAV multispectral imagery. *Remote Sensing Letters*, 9: 933–941. DOI: 10.1080/2150704X.2018.1498600

Kamkar, B., Dashtimarvili, M. & Hosseini, H. (2019) Detection of rice and soybean grown fields and their related cultivation area using Sentinel-2 satellite images in summer cropping patterns to analyze temporal changes in their cultivation area (Case study: four watershed basins of Golestan Province). *Journal of Water and Soil Conservation*, 26: 151–167. DOI: 10.22069/jwsc.2019.15246.3044

Kamkar, B., Dorri, M.A. & Teixeira da Silva, J.A. (2014) Assessment of land suitability and the possibility and performance of a canola (*Brassica napus* L.) – soybean (*Glycine max* L.) rotation in four basins of Golestan province, Iran. *The Egyptian Journal of Remote Sensing and Space Science*, 17: 95–104. DOI: 10.1016/j.ejrs.2013.12.001

Kumral, N.A. & Kovanci, B. (2005) seasonal population dynamics of the two-spotted spider mite, *Tetranychus urticae* Koch (Acari: Tetranychidae) under acaricide constraint on eggplant in Bursa province (Turkey). *Acarologia*, 45: 295–301.

Lamqadem, A.A., Saber, H. & Pradhan, B. (2018) Quantitative assessment of desertification in an arid oasis using remote sensing data and spectral index techniques. *Remote Sensing*, 10. DOI: 10.3390/rs10121862

Lan, Y., Zhang, H., Hoffmann, W.C. & Juan D. Lopez, J. (2013) Spectral response of spider mite infested cotton: Mite density and miticide rate study. *International Journal of Agricultural and Biological Engineering*, 6: 48–52. DOI: 10.3965/j.ijabe.20130601.004

Legendre, P. & Fortin, M.J. (1989) Spatial pattern and ecological analysis. *Vegetatio*, 80: 107–138. DOI: 10.1007/BF00048036

Litskas, V.D., Migeon, A., Navajas, M., Tixier, M.-S. & Stavrinides, M.C. (2019) Impacts of climate change on tomato, a notorious pest and its natural enemy: small scale agriculture at higher risk. *Environmental Research Letters*, 14. DOI: 10.1088/1748-9326/ab3313

Liu, J.M., Wang, H.W., Chang, F.W., Liu, Y.P., Chiu, F.H., Lin, Y.C., Cheng, K.C. & Hsu, R.J. (2016) The effects of climate factors on scabies: A 14-year population-based study in Taiwan. *Parasite*, 23: 1–7. DOI: 10.1051/parasite/2016065

Majeed, M.Z., Javed, M., Riaz, M.A. & Afzal, M. (2016) Population dynamics of sucking pest complex on some advanced genotypes of cotton under unsprayed conditions. *Pakistan Journal of Zoology*, 48: 475–480.

Margolies, D.C. & Wrensch, D.L. (1996) Temperature-induced changes in spider mite fitness: offsetting effects of development time, fecundity, and sex ratio. *Entomologia Experimentalis et Applicata*, 78: 111–118. DOI: 10.1111/j.1570-7458.1996.tb00770.x

Martin, D.E. & Latheef, M.A. (2017) Remote sensing evaluation of two-spotted spider mite damage on greenhouse cotton. *Journal of Visualized Experiments*, 122: 1–9.

Martin, D.E., Latheef, M.A. & López, J.D. (2015) Evaluation of selected acaricides against twospotted spider mite (Acari: Tetranychidae) on greenhouse cotton using multispectral data. *Experimental and Applied Acarology*, 66: 227–245. DOI: 10.1007/s10493-015-9903-6

Meena, N.K., Pal, R., Pant, R.P. & Medhi, R.P. (2013) Seasonal incidence of mite and infuence of pesticidal application on orchid flower production. *Journal of Plant Protection Research*, 53: 124–127. DOI: 10.2478/jppr-2013-0018

Mullan, B., Porteous, A., Wratt, D. & Hollis, M. (2005) *Changes in drought risk with climate change*. NIWA, New Zealand, 58 pp.

Overmars, K.P., de Koning, G.H.J. & Veldkamp, A. (2003) Spatial autocorrelation in multi-scale

land use models. *Ecological Modelling*, 164: 257–270. DOI: 10.1016/S0304-3800(03)00070-X

Rao, K.S., Vishnupriya, R., Ramaraju, K. & Poornima, K. (2018) Effect of abiotic factors on the population dynamics of two spotted spider mite, *Tetranychus urticae* Koch and its predatory mite, *Neoseiulus longispinosus* (Evans) in Brinjal Ecosystem. *Journal of Experimental Zoology*, 21: 797–800.

Reisig, D. & Godfrey, L. (2006) Remote sensing for detection of cotton aphid– (Homoptera: Aphididae) and spider mite– (Acari: Tetranychidae) infested cotton in the San Joaquin valley. *Environmental Entomology*, 35: 1635–1646. DOI: 10.1093/ee/35.6.1635

Romo, C.M. & Tylianakis, J.M. (2013) Elevated temperature and drought interact to reduce parasitoid effectiveness in suppressing hosts. *PLoS ONE* 8: e58136. DOI: 10.1371/journal.pone.0058136

Scott, W.S., Catchot, A., Gore, J., Musser, F. & Cook, D. (2013) Impact of twospotted spider mite (Acari: Tetranychidae) duration of infestation on cotton seedlings. *Journal of Economic Entomology*, 106: 862–865. DOI: 10.1603/EC12333

Soleimany, A., Grubliauskas, R. & Šerevičienė, V. (2021) Application of satellite data and GIS services for studying air pollutants in Lithuania (case study: Kaunas city). *Air Quality, Atmosphere and Health*, 14: 411–429. DOI: 10.1007/s11869-020-00946-z

Stavrinides, M.C. & Mills, N.J. (2011) Influence of temperature on the reproductive and demographic parameters of two spider mite pests of vineyards and their natural predator. *BioControl*, 56: 315–325. DOI: 10.1007/s10526-010-9334-6

Thomas, C. (2001) Biological control of two-spotted spider mite. Integrated Pest Management Program, Pennsylvania Department of Agriculture. *The University of Connecticut, UConn Extension, College of Agriculture, Health and Natural Resources*. Available from: http://ipm.uconn.edu/documents/raw2/html/664.php?aid=664

Vinatier, F., Tixier, P., Duyck, P.-F. & Lescourret, F. (2011) Factors and mechanisms explaining spatial heterogeneity: a review of methods for insect populations. *Methods in Ecology and Evolution*, 2: 11–22. DOI: 10.1111/j.2041-210X.2010.00059.x

Willmott, C.J. (1982) Some comments on the evaluation of model performance. *Bulletin of the American Meteorological Society*, 63: 1309–1313.

Zhang, C. & McGrath, D. (2004) Geostatistical and GIS analyses on soil organic carbon concentrations in grassland of southeastern Ireland from two different periods. *Geoderma*, 119: 261–275. DOI: 10.1016/j.geoderma.2003.08.004

Zhang, C., Zhang, S. & He, J. (1998) Spatial distribution characteristics of heavy metals in the sediments of Changjiang River system - spatial autocorrelation and fractal methods. *Acta Geographica Sinica*, 53: 87–96.

تـأثیر پارامترهـای اقلیمـی بـر جمعیـت کنـۀ تـارتن دو لکـه‌ای (Acari: Tetranychidae) براساس روش سنجش از دور در نواحی جنوب شرقی دریای خزر

محمود جوکار

موسسه تحقیقات پنبه کشور، سازمان تحقیقات، آموزش و ترویج کشاورزی، گرگان، ایران؛ رایانامه: *m.jokar@areeo.ac.ir*

چکیده

کنۀ *Tetranychus urticae* Koch (Acari: Tetranychidae) به عنوان آفت جدی در مزارع پنبه در سراسر جهان شناخته می‌شود. در این پژوهش، پایش جمعیت *T. urticae* با استفاده از داده‌های ماهواره‌ای شاخص پوشش گیاهی و عوامل اقلیمی به صورت سری زمانی و نزدیک به زمان واقعی انجام شد. مطالعه حاضر با هدف تعیین همبستگی بین پویایی جمعیت *T. urticae* با اثرات شاخص آئروسل جذبی (AAI) توسط ماهواره 5-Sentinel، شاخص پوشش گیاهی (m 10) NDVI-Sentinal-2، دما سطح زمین (LST)، تبخیر و تعرق (ET-MODIS)، و بارش (CHIRPS) انجام شد. طغیان کنۀ تارتن همزمان با برداشت گندم در مناطقی که چندین روز گرد و غبار با شاخص آئروسلی زیاد 0/167 ثبت شده بود، مشاهده شد. بارندگی با جمعیت *T. urticae* همبستگی منفی معنی‌داری داشت ($R^2 = 0.378$)، در حالی که سطح آستانه بارش برای تمیز کردن پوشش گیاهی حداقل ۲ میلی‌متر برآورد شد. هیچ الگوی معنی‌داری بین دما و جمعیت *T. urticae* تا اواسط مردادماه ۱۳۹۹ یافت نشد. با این حال، روابط مثبت معنی‌دار در بازه نیمۀ دوم مردادماه تا دهه اول شهریورماه ۱۳۹۹ (هفتگی) مشاهده شد ($R^2 = 0/3519$، 0/1283، 0/1675 و 0/178). تبخیر و تعرق (ET) رابطه مثبت معنی‌دار با پویایی *T. urticae* نشان داد ($R^2 = 0/637$). همچنین بین افزایش NDVI و جمعیت *T. urticae* تا اواسط مردادماه، همبستگی مثبت و سپس از آن به الگوی همبستگی منفی تغییر یافت ($R^2 = 0/273$ و 0/139). بر اساس یافته‌های حاضر، شاخص آئروسل جذبی (AAI) ماهواره-5Sentinel و تبخیر و تعرق ماهواره MODIS، پتانسیل پیش‌بینی جمعیت کنه‌های تارتن را با وضوح زمانی بیشتری داشتند.

واژگان کلیدی: شاخص آئروسل جذبی؛ تبخیر و تعرق؛ شاخص تفاوت پوشش گیاهی نرمال شده؛ سنجش از دور؛ سنتینل-۲ و ۵؛ کنۀ تارتن دو لکه‌ای.

EFFECTS OF CLIMATIC PARAMETERS ON TSSM POPULATION BASED ON REMOTE SENSING